Journal of Biomolecular NMR, **21:** 153–160, 2001.
KLUWER/ESCOM

Measurement of small scalar and dipolar couplings in purine and pyrimidine bases*

Lukáš Žídek[a], Haihong Wu[b], Juli Feigon[b] & Vladimír Sklenář[a,**]
[a]*Masaryk University, Faculty of Science, National Centre for Biomolecular Research, Kotlářská 2, 61137 Brno, Czech Republic;* [b]*University of California, Los Angeles, Department of Chemistry and Biochemistry and Molecular Biology Institute, Los Angeles, California 90024, U.S.A.*

Received 8 June 2001; Accepted 17 July 2001

Key words: NMR methods, nucleic acid bases, residual dipolar couplings, spin-state-selective filters

Abstract

A suite of spin-state-selective excitation (S^3E) NMR experiments for the measurements of small one-bond (^{13}C-^{13}C, ^{15}N-^{13}C) and two-bond (^1H-^{13}C, ^1H-^{15}N) coupling constants in ^{13}C,^{15}N labeled purine and pyrimidine bases is presented. The incorporation of band-selective shaped pulses, elimination of the cross talk between α and β sub-spectra, and accuracy and precision of the proposed approach are discussed. Merits of using S^3E rather than α/β-half-filter are demonstrated using results obtained on isotopically labeled DNA oligonucleotides.

Introduction

The traditional methods of structure determination of biological macromolecules utilize the magnitude of the nuclear Overhauser enhancement (NOE) and values of three-bond scalar coupling constants (^3J) as sources of information to measure short internuclear distances and torsion angles, respectively. Both NOE and ^3J can only relate a nucleus to its neighbors within a few-angstrom vicinity. This limitation does not apply to dipolar interactions. Unlike scalar couplings, dipolar interactions depend on the averaged orientation of the internuclear vectors with respect to the direction of an external magnetic field (Losonczi et al., 1999). With the recent introduction of liquid crystalline media, such as solutions of bicelles (Sanders and Schwonek, 1992; Tjandra and Bax, 1997a) or filamentous phages (Clore et al., 1998; Hansen et al., 1998), residual dipolar couplings can be measured even for molecules with small magnetic susceptibilities.

*This work was supported by Grant No. LN00A016 from Ministry of Education of the Czech Republic.
**To whom correspondence should be addressed. E-mail: sklenar@chemi.muni.cz

The residual dipolar couplings can serve either as restraints in molecular dynamic calculations or as a source of direct information about the geometry of selected fragments of macromolecules. Their application to protein and nucleic acid structure determination was demonstrated immediately after the liquid crystalline media became available (Tjandra et al., 1997, 2000; Ottiger et al., 1997; Clore et al., 1999; Vermeulen et al., 2000). The relationship between one- or two-bond scalar couplings and molecular geometry is much less well understood than in the case of dipolar couplings. Nevertheless, they may provide additional usefull information about studied structures. In this paper, we present spin-state-selective methods designed for measurement of small couplings in nucleic acid bases. The values of the scalar couplings can be obtained directly from the spectra of the sample in isotropic media while residual dipolar couplings are determined as differences between measured total couplings of partially oriented and isotropic samples.

The magnitude of the dipolar coupling constant $^nD = \gamma_i\gamma_j/r_{ij}^3$, where r_{ij} represents an internuclear distance and $\gamma_i\gamma_j$ is a product of magnetogyric constants. Considering that the splitting due to dipolar interactions decreases with cube of the internuclear distance, the one-bond (^1D) and two-bond (^2D) cou-

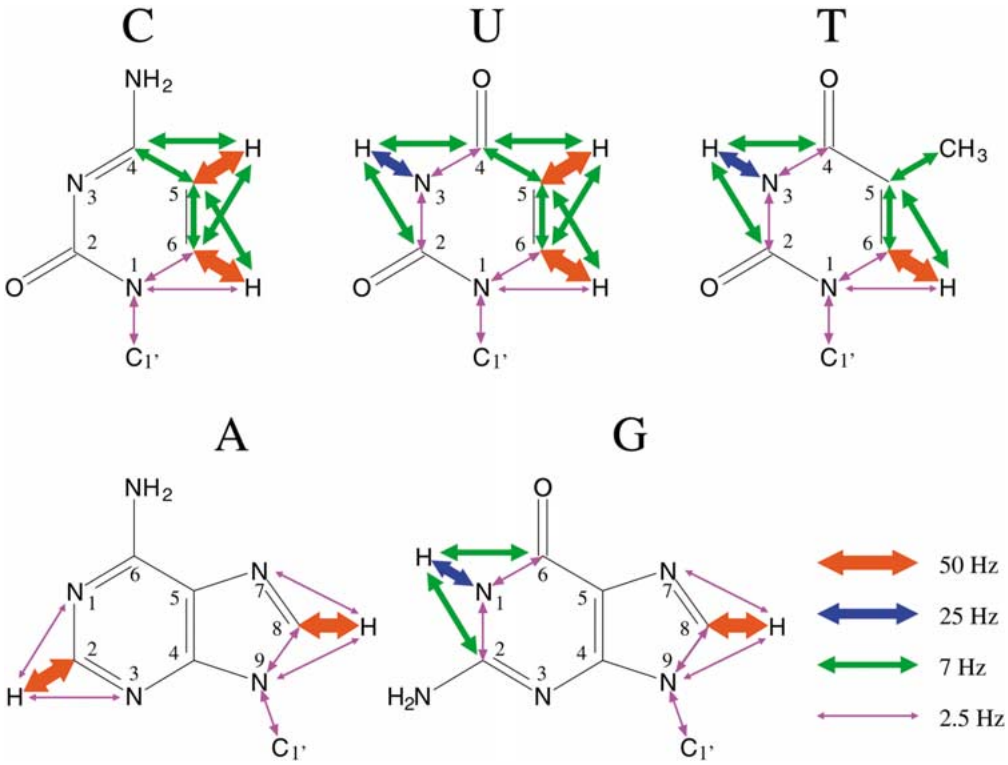

Figure 1. Measurable residual dipolar couplings in nucleic acid bases are marked with arrows. The line thickness represents the upper limit of ^{n}D magnitude. The scale on right is calibrated to a maximal ^{1}D(NH) coupling of 25 Hz (Permi and Annila, 2000).

pling constants are most valuable for structure determination. In addition, the fact that the value of ^{n}D is proportional to the product of the magnetogyric constants of the interacting nuclei suggests that ^{2}D values are too small if the pair of nuclei does not include protons. Figure 1 shows the relative magnitudes of measurable residual dipolar couplings in nucleic acid bases. It should be noted that not all shown dipolar couplings are independent. However, the determination of additional couplings helps to reduce experimental error. Approximate values of the one-bond scalar couplings are 175–215 Hz (CH), 85 Hz (NH), 50–70 Hz (CC), and 8–19 Hz (NC). The two-bond couplings are less than 5 Hz, with the exception of the purine ^{2}J(NH), which are 8–15 Hz (Ippel et al., 1996, and results obtained in this study).

Materials and methods

The relevant scalar and dipolar couplings in nucleic acids are summarized in Figure 1. The small size of the two-bond couplings and fast relaxation characteristics of larger nucleic acid molecules require carefull design of the pulse sequence for optimal sensitivity. Figure 2A demonstrates the general experimental approach used in this study. The pulse sequences contain the spin state selective excitation (S^3E) element (Meissner et al., 1997a,b) and resemble experiments designed to measure coupling constants in proteins (Meissner et al., 1998). Following the terminology of Wang and Bax (1995), the experiment will be referred to as IS[T] in this paper. The sequence shown in Figure 2 is similar to experiments designed by Permi and coworkers (Permi et al., 1999; Permi and Annila, 2000) for measurement of residual dipolar couplings in the protein backbone. The latter sequences differ in the choice of the spin-state selective filter, using the long α/β-half filter (Andersson et al., 1998) rather than the S^3E element. Figure 2B shows the long α/β-half filter modified for measurements of nucleic acids by introduction of the necessary selective pulses. The performance of both types of experiments are compared below.

The S^3E experiments have been described in great detail in the literature (Meissner et al., 1997a,b). Therefore, the basic features will be only briefly men-

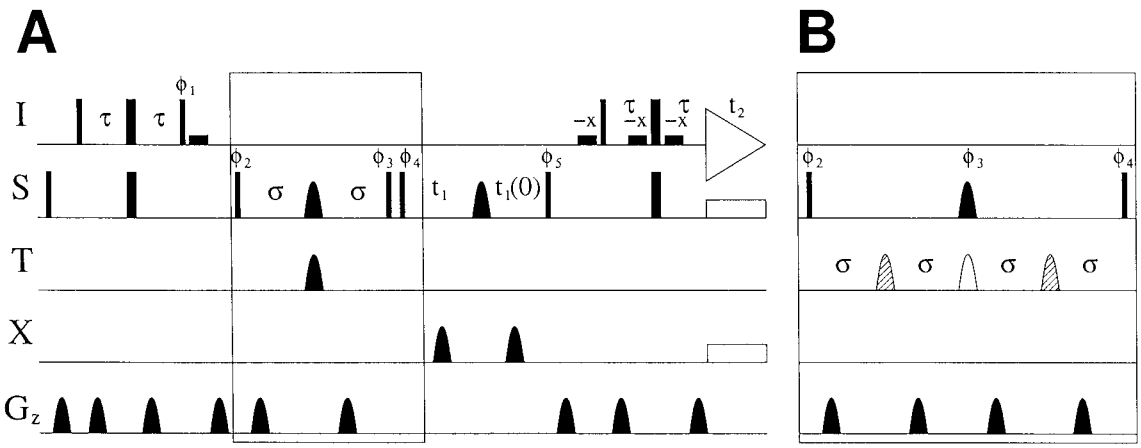

Figure 2. S^3E IS[T] pulse sequence (A). Narrow and wide bars indicate hard $\pi/2$ and π pulses, respectively. Round shapes represent selective π pulses described in the text. Water-selective $\pi/2$ pulses are indicated with small rectangles. Open rectangles represent decoupling during acquisition. The pulses were applied with phase x unless otherwise indicated. Two subspectra were recorded using phase cycling ϕ_1 = 4(y), 4(−y); ϕ_2 = 2(x+π/4); ϕ_3 = x, y; ϕ_4 = x, y; ϕ_5 = x, ϕ_{rec} = x, 2(−x), x; and ϕ_1 = 4(y), 4(−y); ϕ_2 = x + π/4, x + 5π/4; ϕ_3 = x, y; $\phi_4 = -x, -y$; ϕ_{rec} = x, 2(−x), x; with ϕ_5 incremented in the States-TPPI manner (Marion et al., 1989). The subspectra were subtracted and added to obtain α and β spectra (Meissner et al., 1997a). The delays were τ = 1/(4J(IS)) and σ = 1/(8J(ST)). The sine-shaped 0.8 ms pulse-field gradients were applied with the respective strengths of 47, 11, 11, 13, 5, 5, 35, 32, and 32 G/cm. The S^3E element, shown in a box, can be replaced with the α/β-half-filter (B; Andersson et al., 1998; Permi et al., 1999). In the α/β-half-filter version, antiphase and in-phase subspectra were recorded using phase cycling ϕ_1 = 4(y), 4(−y); ϕ_2 = x, −x; ϕ_3 = x; ϕ_4 = 2(x), 2(−x); ϕ_5 = y; ϕ_{rec} = 2(x, −x), 2(−x, x); and ϕ_1 = 4(y), 4(−y); ϕ_2 = x, −x; ϕ_3 = x; ϕ_4 = 2(y), 2(−y); ϕ_5 = x; ϕ_{rec} = 2(x, −x), 2(−x, x), respectively. Open and hatched shaped pulses were only used when recording antiphase and in-phase spectra, respectively. Phases ϕ_2, ϕ_3, and ϕ_4 were incremented in the States-TPPI manner. The subtraction and addition of the antiphase and in-phase subspectra yielded α and β spectra corresponding to those obtained using the pulse sequence A.

tioned here. The magnetization is transferred from the excited proton I to the nucleus S during the first INEPT. The following S^3E element allows the coupling to the nucleus T to evolve and cycling of the phases ϕ_4 and ϕ_5 separates the resulting magnetization described by operators $S_x T^\alpha = S_x(1/2 + T_z)$ and $S_x T^\beta = S_x(1/2 - T_z)$. The receiver cycling then selects either the T^α or T^β state and two subspectra are recorded in the interleaved manner (Meissner et al., 1997a,b). If the nucleus T is kept coupled during the t_1 evolution and acquisition, the T^α and T^β subspectra contain peaks shifted in both dimensions by the coupling constants. The overlaid spectra thus provide the typical E. COSY pattern without introducing possible overlaps by doubling the number of peaks like in the regular E. COSY spectra.

While the T nucleus must not be perturbed after selection, as described, decoupling of other nuclei interacting with S (abbreviated X in Figure 2) is important in order to obtain narrow and well-defined peaks. Due to the requirement for selective excitation and decoupling, attention must be paid to a careful choice of selective pulses when the general pulse scheme in Figure 2 is applied to particular I–S–T groups. Fortunately, for nucleic acid bases the chemical shift values allow the necessary distinction between the nuclei of interest. The selective pulses (pulse length, shape, frequency) utilized in the IS[T] experiments for purine and pyrimidine bases are summarized in Table 1.

Dipolar couplings involving exchangeable imino protons contain important structural information, especially in the case of guanine (Figure 1). Therefore, the IS[T] experiment must provide efficient suppression of the water resonance. It is achieved by employing the water flip-back (Grzesiek and Bax, 1993) and the WATERGATE element (Piotto et al., 1992) in the sequence depicted in Figure 2A. Although using two sets of samples, dissolved in D_2O and H_2O, would limit the need for water suppression to a small subset of the experiments, all of the presented experiments are designed to be applicable to H_2O samples.

The most straightforward application of the pulse sequence shown in Figure 2A is a measurement of couplings in H–C–N groups. The HC[N] experiment provides values of ^1D(N1C1′), ^1D(N1C6), and ^2D(N1H6) in pyrimidines and of ^1D(N9C1′), ^1D(N9C8), and ^2D(N9H8) in purines. Values of ^1D(N7C8) in purines and of ^1D(N1C2) and

Table 1. Selective pulses utilized in the IS[T] experiments

Experiment	Spin state selection	Decoupling in t_1	Decoupling in t_2
HC[N]			
T=N1/N9	2 ms IBURP-2, 157 ppm	2 ms IBURP-2, 225 ppm (N7)	select.[a], 225 ppm (N7)
S=C1′	2.5 ms REBURP, 85 ppm	1.5 ms Q3, 35 ppm (C2′)	nonsel. GARP on ^{13}C
S=C6	2.5 ms REBURP, 140 ppm	1.5 ms Q3, 96 ppm (C5)	nonsel. GARP on ^{13}C
S=C8	2.5 ms REBURP, 138 ppm	1.5 ms Q3, 159 ppm (C4+C6)	nonsel. GARP on ^{13}C
HN[C]			
S=N3/N1	nonsel. on ^{15}N	1.5 ms Q3, 74 ppm (N2[b])	nonsel. on ^{15}N
T=C2 (U,T)	5 ms Q3, 154 ppm	5 ms Q3, 169 ppm (C4[c])	not applied
T=C4 (U,T)	5 ms Q3, 169 ppm	5 ms Q3, 154 ppm (C2[c])	not applied
T=C2 (G)	5 ms Q3, 156 ppm	5 ms Q3, 161 ppm (C6)	not applied
T=C6 (G)	5 ms Q3, 161 ppm	5 ms Q3, 156 ppm (C2)	not applied
HN[H]			
S=N7	nonsel. on ^{15}N	not applied	nonsel. GARP on ^{15}N
S=N1	275 μs rect., 223 ppm	1 ms IBURP-2, 84 ppm (N6[b])	nonsel. GARP on ^{15}N
S=N3	128 μs rect., 215 ppm	2 ms IBURP-2, 170 ppm (N9[b])	nonsel. GARP on ^{15}N
HC[C]			
S=C6, T=C5	1.55 ms Q3[d], 96+140 ppm	not applied	select.[a], 140 ppm (C6)
S=C5, T=C6	1.55 ms Q3[d], 96+140 ppm	2 ms IBURP-2, 167 ppm (C4)	select.[a], 96 ppm (C5)
S=C5, T=C4	1.5 ms Q3[d], 96+167 ppm	2 ms IBURP-2, 140 ppm (C6)	select.[e], 157 ppm (C5+C6)

[a]2 ms IBURP-2 incorporated into MLEV-4.
[b]Inter-base couplings in base pairs can be decoupled simultaneously using phase-modulated pulse..
[c]Phase-modulated 2 ms Q3 can be used to decouple C5 simultaneously.
[d]Phase-modulated to achieve dual excitation.
[e]0.55 ms IBURP-2 incorporated into MLEV-4.

^1D(N3C2) in adenine cannot be obtained from the HC[N] experiment due to small ^1J(NC) values (less than 3 Hz, Ippel et al., 1996). Selective 2 ms IBURP-2 (Geen and Freeman, 1991) pulses were applied on nitrogen at 157 and 225 ppm in order to select N1/N9 and decouple N7 (during t_1 and t_2), respectively. The selective refocusing of C6/C8 was achieved by a 2.5 ms REBURP (Geen and Freeman, 1991) pulse while a 1.5 ms Gaussian cascade Q3 (Emsley and Bodenhausen, 1990) was used to decouple C2′, purine C4 and C6, and pyrimidine C5.

The HN[C] experiment was designed for measuring of ^1D(NC) and ^2D(CH) couplings in H–N–C groups of thymine, uracil, and guanine. The relatively close chemical shift values of C4 (169 ppm) and C2 (154 ppm) in thymine and uracil and of C6 (161 ppm) and C2 (156 ppm) in guanine represent a challenge for selective carbon pulses. We were able to achieve selective excitation using a 5 ms Gaussian cascade Q3 (Emsley and Bodenhausen, 1990). The long inversion pulse is compatible with the length of the S^{3}E element set for the ^1J(NC) values being lower than 20 Hz (Ippel et al., 1996). Carbon decoupling in t_1 can be also achieved by the Q3 cascades. Phase modulation of the decoupling Q3 pulse allows simultaneous inversion of the carbon adjacent to the imino group and of C5 (^2J(N1C5) = 5.7 Hz in uracil (Ippel et al., 1996)). The unique chemical shifts of imino nitrogen make selection of nitrogens easy. Furthermore, N2 and N3 of guanine and N1 of pyrimidines cause only small, approximately 2 Hz, splitting of lines of imino nitrogens (Ippel et al., 1996). On the other hand, the hydrogen-bonded nitrogens to the imino group exhibit higher ^{2h}J(N1N3) values and are worthy of decoupling (Dingley et al., 1999).

The HN[H] experiment allows measurement of the ^2D(N1H2), ^2D(N3H2), and ^2D(N7H8) coupling constants in purines. These couplings cannot be obtained from the HC[N] experiment due to the very small ^1J(NC) values as discussed above. Fortunately, large ^2J(NH) values allow the magnetization transfer from protons directly to nitrogens during the first INEPT step (Figure 2A). Note that the first τ should be set to $1/8\,^2J$(NH) in the case of T = H2, which is coupled to two practically indistinguishable nitrogens N1 and N3. In practice, τ periods shorter than $1/4\,^2J$(NH) are also used for T = H8 in order to reduce relaxation during the INEPT transfers. It should be emphasized that H2

and H8 act as both I and T nuclei in this version of the IS[T] experiment. As a consequence, the E. COSY pattern is not observed and the peaks in the individual spectra are displaced only in the indirect dimension. This displacement provides the ^2D(NH) value. In the ^2D(N1H2) and ^2D(N3H2) measurements, the interfering N6 and N9 nuclei can be distinguished easily from N1 and N3 by using selective rectangular pulses because the differences between N1 vs. N6 and N3 vs. N9 chemical shift differences are large. IBURP-2 pulses (Geen and Freeman, 1991) are used for N6 and N9 decoupling in t_1 while all carbons are decoupled in during t_1 and t_2. HN[H] (and analogous HC[H]) experiments are obviously applicable to measurements of one-bond dipolar couplings as well. However, large values of ^1J(CH) and ^1J(NH) usually do not require spin-state-selective experiments.

The ^1D(CC) and ^2D(CH) couplings at positions 5 and 6 in pyrimidines can be obtained using the HC[C] version of the pulse sequence in Figure 2A. Gaussian cascades Q3 (Emsley and Bodenhausen, 1990) applied to S and T and IBURP-2 (Geen and Freeman, 1991) applied to X provided good selection and decoupling during the t_1 period, respectively. Decoupling of C6 in the ^2D(C5H6) measurement and of C6 and C5 in the ^2D(C5H4) measurement was achieved by using IBURP-2 pulses of 2 ms and 0.55 ms, respectively, incorporated into a MLEV-4 pulse train (McCoy and Mueller, 1993). Only C5 was decoupled during the measurement of ^2D(C6H5) because the value of ^2J(C4H5) is less than 2 Hz (Ippel et al., 1996). Homonuclear proton decoupling during acquisition (Vander Kooi et al., 1999), although not used in this study, would certainly be beneficial because of ^3J(H5H6) being relatively strong (approximately 7 Hz, Ippel et al., 1996).

Higher values of ^1J(CC) utilized by the selection filters offer more straightforward alternatives. A constant-time HSQC-E. COSY experiment can be used for the ^2D(CH) measurements when sensitivity and spectral overlaps do not represent a serious problem. The duration of the constant-time evolution can be kept relatively short to limit relaxation. Sufficient ^{13}C selectivity can be achieved using 0.75 ms Sinc $\pi/2$ and Seduce π pulses (McCoy and Mueller, 1992). The ^1D(CC) coupling constants are then measured separately by an HSQC experiments allowing the ^1J(CC) coupling to evolve in the t_1 period.

The IS[T] experiments were tested on a uniformly ^{13}C,^{15}N-labeled DNA hairpin d(GCGAAGC) and a DNA duplex [d(CGTTTTAAAACG)]$_2$. Figure 3 shows guanine regions of HC[N] and HN[H] spectra of 0.2 mM [d(CGTTTTAAAACG)]$_2$ dissolved in 25 mM ammonium chloride, pH 6.0, containing 11 mg/ml bacteriophage Pf1 (Hansen et al., 1998) and 20 % deuterium oxide as examples.

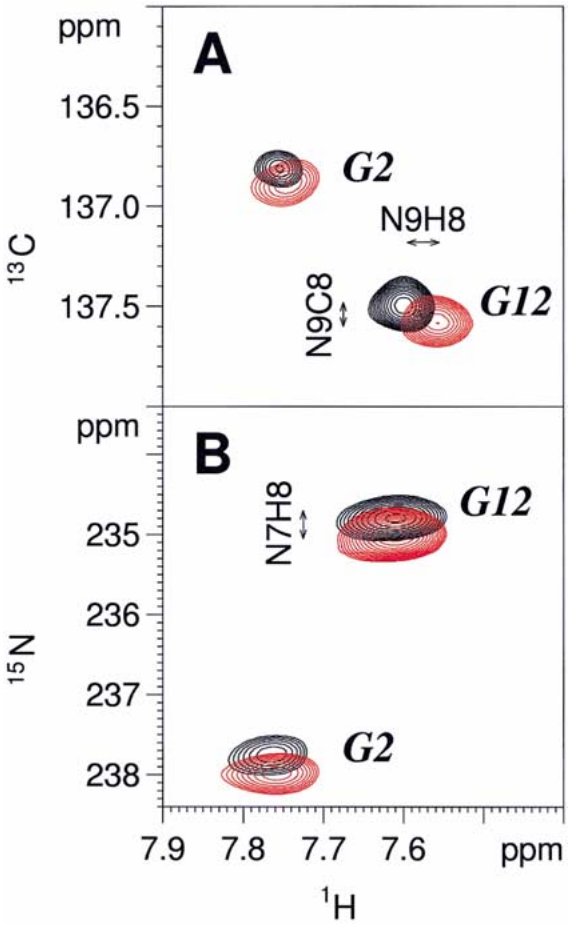

Figure 3. Guanine regions of S^{3}E HC[N] (A) and HN[H] (B) spectra of partially aligned [d(CGTTTTAAAACG)]$_2$. Individual subspectra, shown in black and red, are overlaid. The spectra were recorded at 15°C in a Shigemi tube on a 500 MHz Bruker Avance spectrometer equipped with a 5 mm triple resonance TXI H-C/N-D z-gradient probe. In both experiments, 40 (F_1) and 600 (F_2) points were obtained, apodized with the squared cosine function, and zero filled to 512 (F_1) and 8192 ((F_2) points. Spectral widths of 5 kHz in F_2 and 503 Hz in F_1 (A) and 9 kHz in F_2 and 405 Hz in F_1 (B) were used. Signal-to-noise ratios of guanine 2 and guanine 12 peaks, respectively, were 3.5 and 6.5 in spectrum A (512 scans, 16 hours), and 4.0 and 5.5 in spectrum B (3072 scans, 90 hours).

Results and discussion

The small values of some of the measured dipolar coupling constants requires careful control of the accuracy

and precision of the described experiments. When the selected α and β peaks are not resolved to the baseline, an occurrence of the undesired component of the doublet leads to underestimation or overestimation of the coupling. One reason for the presence of such undesired component is the change of the state of the passive spin (T) between t_1 and t_2 (Wang and Bax, 1996; Sørensen et al., 1999). This effect is likely to be small in most experiments because the passive nuclei in the relevant HC[N] and HN[C] experiments are slowly relaxing unprotonated carbons and nitrogens. ^2J(CH) couplings obtained from the HC[C] experiment can be corrected for the passive spin flip as described in literature (Wang and Bax, 1996; Meissner et al., 1998; Sørensen et al., 1999). However, the effect of the passive spin flip will be small for the HC[C] experiment in comparison with pulse sequences discussed in the cited references thanks to significantly shorter period between t_1 and t_2. Another source of the unwanted peaks in the spectra is a difference between the actual value of coupling and the value of J(ST) used for setting the σ delay (Figure 2A). Intensity of the undesired peak relative to the intensity of the desired peak equals to $-\tan((\pi/4)(8J\sigma - 1))$ for filters of duration equal to 1/4J(ST) and to $\tan^2((\pi/4)(8J\sigma - 1))$ for filters of duration equal to 1/2J(ST) (Sørensen et al., 1997; Andersson et al., 1998). Fortunately, the undesired cross-talk peaks can be eliminated by an appropriate linear combination of the subspectra (Meissner et al., 1998).

The accuracy of the S^3E IS[T] scheme was studied on HC[N] spectra of 1 mM d(GCGAAGC) DNA hairpin in isotropic phase and compared to the analogous experiment employing the long α/β-half-filter (Andersson et al., 1998; Permi et al., 1999). A set of HC[N] spectra was measured for σ = 14.92, 13.19, 11.80, 10.66, 9.72, and 8.92 ms. These σ values were experimentally corrected for the evolution of in-phase and anti-phase coherences during the selective REBURP and IBURP-2 pulses (total length of an echo involving the selective pulses was calibrated using ^{13}C-labeled sodium acetate). The apparent couplings were determined as displacements of the corresponding α and β peaks picked automatically by the Sparky 3.87 software (University of California, San Francisco). The measured values (open circles, Figure 4) exhibited a strong anticorrelation with the values used for the σ setting. Although the measured displacements strongly deviated from the actual coupling, the ^1J(N9C8) value was easily obtained as the intercept of the displacement plot with the diagonal. Figure 4 demonstrates that linear combination of subspectra allowed extrapolation of the apparent couplings to their actual values obtained for σ = 13.19 ms (crosses) and σ = 9.72 ms (dots). The correction was performed by a linear combination of subspectra in a ratio of $1 : \tan((\pi/4)(J^*/J_0 - 1))$, where $J_0 = 1/8\sigma$ and J^* is the expected actual value of ^1J(N9C8), varied in the course of extrapolation. Such correction provided couplings identical to the measured ones within the experimental error for both values of σ. Identical values were also obtained using the long α/β-half-filter. It should be noted that the effect of uncorrect σ setting was smaller for the long α/β-half-filter (Sørensen et al., 1997; Andersson et al., 1998), but not negligible. Correction of the measured peak displacement is thus required for both spin-state-selective elements. The fact that the dependence of measured peak displacement on $J_0 = 1/8\sigma$ is almost linear for the S^3E IS[T] (Figure 4) makes the short S^3E element favorable (Figure 2A). Couplings measured by HC[N] and HN[H] experiments were compared to the values obtained from *J*-modulated constant-time HSQC spectra (Tjandra and Bax, 1997b). No systematic differences were observed between the IS[T] and *J*-modulated HSQC experiments (Figure 5), indicating good extrapolation to actual *J* values and negligible effect of the passive spin flip.

HC[N] spectra of 1 mM d(GCGAAGC) were also used to estimate the precision of the measurements. From a series of five quick (24 scans, 1.5 hour) experiments, standard deviations of ^1J(N9C8) ranging from 0.12 Hz (guanine 6, S/N = 18) to 0.48 Hz (guanine 1, S/N = 8) were obtained. The two-bond ^2J(N9H8) couplings were measured with similar precision (standard deviation ranging from 0.15 Hz to 0.24 Hz). These results show that a precision close to 0.1 Hz can be achieved for a signal-to-noise ratio of 20. The dependence of the standard deviation on the signal-to-noise ratio demonstrates that high sensitivity is necessary for precise measurement of small couplings. While no significant difference in sensitivity was found in d(GCGAAGC) spectra, the spectra of $[d(CGTTTTAAAACG)]_2$ were recorded with approximately two times higher sensitivity using S^3E HC[N] experiment compared to the version employing the long α/β-half-filter.

Our experience thus show that similar accuracy can be achieved using either S^3E or a long α/β-half-filter but higher sensitivity makes S^3E IS[T] the experiment of choice. Applicability of the presented method to measurement of various couplings was tested on sam-

Table 2. Scalar and residual dipolar couplings measured for selected bases of d(GCAAGC)

Coupling		Cytosine 2		Cytosine 7		Adenine 4		Guanine 3		Guanine 6	
Pyrim.	Purine	J (Hz)	D (Hz)	J (Hz)	D (Hz)	J (Hz)	D (Hz)	J (Hz)	D (Hz)	J (Hz)	D (Hz)
C5H5	C2H2			174.8	−3.9	201.4	3.9				
C6H6	C8H8	180.6	−12.6	181.7	−9.1	213.3	8.8	214.7	0.2	213.9	−11.5
N3H3	N1H1									−87.2	9.8
C5C6		66.7	−3.1	69.3	−1.2						
N1C1′	N9C1′	(−12.9)[a]	(−0.1)[a]	−11.7	−0.5	(−12.7)[a]	(1.2)[a]			−11.5	−0.4
N1C6	N9C8	−12.5	−0.5	−12.8	0.2	−11.4	0.4	−10.6	0.6	−10.7	−0.5
	N1C2									(−13.9)[b]	(−0.3)[b]
	N1C6									(−12.7)[b]	(−0.5)[b]
C5H6		1.6	−0.7	3.0	0.7						
	C2H1									(0.5)[b]	(−2.0)[b]
	C6H1									(0.0)[b]	(−3.0)[b]
N1H6	N9H8	−1.9	0.1	−1.6	0.6	−6.1	−0.8	−7.1	0.3	−6.8	−0.2
	N7H8					−11.6	−0.6	−11.5	0.1	−11.4	1.0
	N3H2					−14.6	−0.5				
	N1H2					−15.3	1.0				

[a]Measured value affected by spectral overlap.
[b]Measured value affected by low peak intensity due to exchange of imino protons.

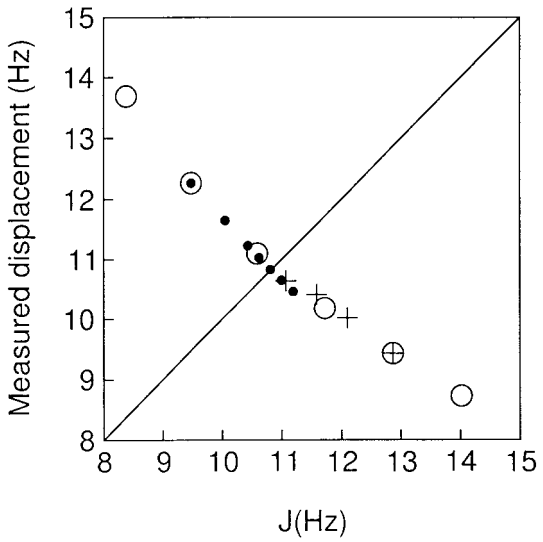

Figure 4. Dependence of apparent values of ^1J(N9C8), measured as peak displacement, on values of ^1J(N9C8) used for setting σ in the S^{3}E HC[N] experiment (open circles). Dots and crosses represent series of extrapolated values obtained by correction of S^{3}E spectra obtained for σ = 13.19 ms and 9.72 ms, respectively. The correction was performed by linear combination of subspectra in a ratio of 1 : $\tan((\pi/4)(J^*/J_0 - 1))$, where $J_0 = 1/8\sigma$ and J^* is the expected actual value of ^1J(N9C8), varied in the course of extrapolation.

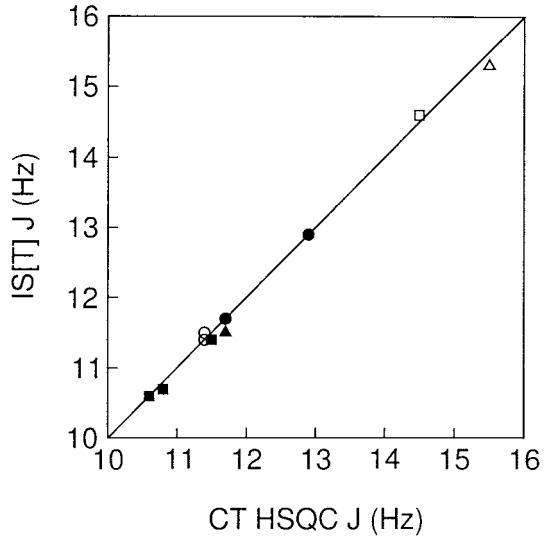

Figure 5. Plot of ^1J(N9C8) (filled circles), ^1J(N1C1′) (filled squares), ^1J(N9C1′) (filled triangles), ^2J(N7H8) (open circles), ^2J(N1H2) (open square), and ^2J(N3H2) (open triangle) obtained by J-modulated constant-time HSQC and IS[T] experiments.

ples of 0.5 mM GCGAAGC dissolved in the isotropic phase and in the presence of the Pf1 phage at concentration causing splitting of the HDO line by 20 Hz. The results are listed in Table 2 for five selected residues (low signal intensities of terminal guanine 1 and flexible adenine 5 did not allow reliable measurements). In this small hairpin, imino protons are in relatively fast exchange and the precision of couplings involving imino protons is poor due to the low signal intensity. Measurements of couplings involving H5 of cytosines

are not presented here because their frequencies are very close to the frequency of the solvent. For the sake of completeness, Table 2 also contains one-bond CH and NH couplings, measured from coupled HSQC spectra. Utilization of the measured dipolar couplings in the hairpin structure refinement will be published elsewhere.

Conclusions

In conclusion, a set of experiments for measuring scalar and residual dipolar couplings in nucleic acids was designed and successfully tested on both a DNA hairpin and a duplex. The short spin-state-selective excitation element provided significantly higher sensitivity for measurements of small scalar couplings.

Acknowledgements

The authors thank Sapna Ravindranathan and Petr Padrta for providing spectra assignments.

References

Andersson, P., Weigelt, J. and Otting, G. (1998) *J. Biomol. NMR*, **12**, 435–441.

Clore, G.M., Starich, M.R., Bewley, C.A., Cai, M.L. and Kuszewski, J. (1999) *J. Am. Chem. Soc.*, **121**, 6513–6514.

Clore, G.M., Starich, M.R. and Gronenborn, A.M. (1998) *J. Am. Chem. Soc.*, **120**, 10571–10572.

Dingley, A.J., Masse, J.E., Peterson, R.D., Barfield, M., Feigon, J. and Grzesiek, S. (1999) *J. Am. Chem. Soc.*, **121**, 6019–6027.

Emsley, L. and Bodenhausen, G. (1990) *Chem. Phys. Lett.*, **165**, 469–476.

Geen, H. and Freeman, H. (1991) *J. Magn. Reson.*, **93**, 93–141.

Grzesiek, S. and Bax, A. (1993) *J. Am. Chem. Soc.*, **115**, 12593–12594.

Hansen, M.R., Mueller, L. and Pardi, A. (1998) *Nat. Struct. Biol.*, **5**, 1065–1074.

Ippel, J.H., Wijmenga, S.S., deJong, R., Heus, H.A., Hilbers, C.W., deVroom, E., vanderMarel G.A. and vanBoom, J.H. (1996) *Magn. Reson. Chem.*, **34**, S156–S176.

Losonczi, J.A., Andrec, M., Fischer, M.W.F. and Prestegard, J.H. (1999) *J. Magn. Reson.*, **138**, 334–342.

Marion, D., Ikura, M., Tschudin, R. and Bax, A. (1989) *J. Magn. Reson.*, **85**, 893–899.

McCoy, M.A. and Mueller, L. (1992) *J. Am. Chem. Soc.*, **114**, 2108–12.

McCoy, M.A. and Mueller, L. (1993) *J. Magn. Reson. A*, **101**, 122–130.

Meissner, A., Duus, Ø. and Sørensen, O.W. (1997a) *J. Magn. Reson.*, **128**, 92–97.

Meissner, A., Duus, Ø. and Sørensen, O.W. (1997b) *J. Biomol. NMR*, **10**, 89–94.

Meissner, A., Schulte-Herbrüggen, T. and Sørensen, O.W. (1998) *J. Am. Chem. Soc.*, **120**, 3803–3804.

Ottiger, M., Tjandra, N. and Bax, A. (1997) *J. Am. Chem. Soc.*, **119**, 9825–9830.

Permi, P. and Annila, A. (2000) *J. Biomol. NMR*, **16**, 221–227.

Permi, P., Heikkinen, S., Kilpeläinen, I. and Annila, A. (1999) *J. Magn. Reson.*, **140**, 32–40.

Piotto, M., Saudek, V. and Sklenář, V. (1992) *J. Biomol. NMR*, **2**, 661–665.

Sanders, C.R. and Schwonek, J.P. (1992) *Biochemistry*, **31**, 8898–8905.

Sørensen, M.D., Meissner, A. and Sørensen, O.W. (1997) *J. Biomol. NMR*, **10**, 181–186.

Sørensen, M.D., Meissner, A. and Sørensen, O.W. (1999) *J. Magn. Reson.*, **137**, 237–242.

Tjandra, N. and Bax, A. (1997a) *Science*, **278**, 1111-1114.

Tjandra, N. and Bax, A. (1997b) *J. Magn. Reson.*, **124**, 512–515.

Tjandra, N., Omichinski, J.G., Gronenborn, A.M., Clore, G.M. and Bax, A. (1997) *Nat. Struct. Biol.*, **4**, 732–738.

Tjandra, N., Tate, S., Ono, A., Kainosho, M. and Bax, A. (2000) *J. Am. Chem. Soc.*, **122**, 6190–6200.

Vander Kooi, C.W., Kupče, Ē., Zuiderweg, E.R.P. and Pellecchia, M. (1999) *J. Biomol. NMR*, **15**, 335–338.

Vermeulen, A., Zhou, H. and Pardi, A. (2000) *J. Am. Chem. Soc.*, **122**, 9638–9647.

Wang, A.C. and Bax, A. (1995) *J. Am. Chem. Soc.*, **117**, 1810–1813.

Wang, A.C. and Bax, A. (1996) *J. Am. Chem. Soc.*, **118**, 2483–2494.